8

Equilibrium Phase Diagrams

CHAPTER PREVIEW

Most ceramics are multicomponent materials, and the most stable phase at any temperature is the one with the lowest free energy, *G*. One use of phase diagrams is to represent which phase or phases we might expect to be present as a function of temperature. There are a large number of books concerned with just this one topic. Lots of work was carried out in the 1950s and 1960s, but many systems have remained almost completely unexplored; and it's not a well-funded topic in the United States now. The lack of effort is in spite of the demonstration that new complex ceramics such as the high-temperature superconductors YBCO and BiSCCO and the magnetic manganates possess extraordinary, and potentially very useful, properties.

Much of the classical work on phase equilibria has actually been concerned with processing metals. Thus, the Fe–O phase diagram is perhaps the most thoroughly characterized because of its importance to the iron and steel industry.

A word to keep in mind throughout our discussion is equilibrium: we are talking about equilibrium phase diagrams. Often we use a phase diagram as a guide to processing. If the process is in progress, then it is not in equilibrium. Also, by definition, a chemical reaction is not an equilibrium process. If a reaction is exothermic, then a rise in temperature favors the reactants. Although most of the phase diagrams we use in ceramics are for a pressure of 1 atm, in one-component systems such as carbon pressure is a very important variable. It tells us what pressure we need for direct synthesis of diamond. In metal–oxygen diagrams, the partial pressure of oxygen determines what is the stable form of the oxide.

8.1 WHAT'S SPECIAL ABOUT CERAMICS?

As many ceramics are oxides, the oxygen partial pressure, pO_2, is an important variable. There is a lot of information about many metal–oxygen systems. In part, this is due to interest in how to obtain metals by direct reduction from their oxides. A frequent way of representing free energies of formation of oxides as a function of pO_2 and T is the Ellingham diagram (Ellingham 1944) that was popularized by Richardson and Jeffes for iron and steel production (Richardson and Jeffes 1948). Much less is known about nitrides and oxynitrides or even carbides.

Many ceramics are multicomponent materials, and hence many of the important phase diagrams involve three or more components. Here are some examples of where phase diagrams have very practical applications in the use of ceramics.

Refractory silica brick. It was used for the roof of the open-hearth furnace, which was once an important method for steel production. Now silica refractories are used in coke ovens and as roofs in glass tanks. Typical operating temperatures are 1,625–1,650°C. The phase diagram tells us that the SiO_2 needs to be quite pure (only 0.2–1.0 wt.% Al_2O_3) or it melts.

Fire-clay brick. This is a classic clay product with a composition close to kaolinite. Although it is used at temperatures below 1,587°C, the phase diagram tells us that some liquid is often present because these ceramics contain 22–33 wt.% Al_2O_3. Why is this material so important? It performs the task very well and is cheap to produce.

Barium titanate. Pure cubic $BaTiO_3$ single crystals cannot be grown from a melt of that composition because the hexagonal phase is in equilibrium with the liquid at the solidification temperature (1,618°C). Although the hexagonal phase transforms to the cubic phase at 1,460°C,

DALTON'S LAW OF PARTIAL PRESSURES:

$$p_A = X_A P$$

p_A partial pressure of A
X_A mole fraction of A
P total pressure of gas mixture

C.B. Carter and M.G. Norton, *Ceramic Materials: Science and Engineering*,
DOI 10.1007/978-1-4614-3523-5_8,

the phase change is sluggish and thus the hexagonal phase can exist at room temperature. The hexagonal form of $BaTiO_3$ is not ferroelectric, which is the property we are most often interested in. In Chapter 28 we describe how single crystals of cubic $BaTiO_3$ can be grown.

Adhesion of metals in integrated circuits. Aluminum has been used for over 30 years as interconnect and top-level metallization in integrated circuits. One of the reasons Al is so good is that it reduces SiO_2 to form interfacial metal–oxide bonds that promote adhesion and stability. One of the problems with copper metallizations is that SiO_2 is more stable than Cu_2O. Despite this difficulty, Cu has several significant advantages over Al and is now used in many commercial devices such as IBM's processor for the Apple G5, Intel's Pentium IV, and AMD's Athlon. The relative oxidizing powers of metals are represented frequently on Ellingham diagrams. In Chapter 15 we show how these diagrams can be useful in developing brazes for ceramics.

8.2 DETERMINING PHASE DIAGRAMS

We refer you to basic thermodynamics texts for the details on the origin of phase diagrams and the phase equilibria book by Bergeron and Risbud. In this section we just summarize some key points. First is some thermodynamic background to phase diagrams.

- The phase with the lowest free energy, G, is thermodynamically stable.
- The chemical potential, μ_i, of a component is the same in all of the phases in which it is present. This requirement is used in the derivation of Gibbs Phase Rule.
- At equilibrium, the temperatures and pressures of all phases are equal.

Determining a phase diagram requires measuring which phases are in equilibrium under well-defined conditions. An especially critical factor for ceramics is being sure that we have equilibrium. In ceramics we have two challenges.

- We need to make measurements at high temperature, where direct determination of phases is difficult.
- The valence of the cations may change as the temperature or pressure changes. If the cation is polyvalent, then the valence depends on the oxygen activity, which as we'll see later depends on the partial pressure of oxygen, pO_2.

To ensure that we have equilibrium, the two bulk phases should really be in intimate contact, separated by a flat (planar) interphase boundary.

The number of techniques we can use for direct determination of phase diagrams of ceramic systems is quite limited because of the requirement for high temperatures.

- High-temperature X-ray diffraction. Maximum operating temperatures are up to 2,500°C in high vacuum, 2,400°C in inert atmospheres, and 1,700°C in air.
- Transmission electron microscopy with hot-stage. Maximum temperature 1,300°C; working in vacuum, typically $\sim 10^{-4}$ Pa, so no control of pO_2.

Most techniques that are used to determine phase diagrams experimentally use an indirect approach. Note that often we are not trying to determine an entire diagram but, rather, the specific parts that may be of interest, such as the solvus lines, the liquidus, or the eutectic temperature. Figure 8.1 is an example of using cooling curves to determine the liquidus and eutectic for a binary system. Heating curves produce similar results and are often easier to achieve experimentally. Phase changes produce the deviations in time–temperature curves. These measurements would be made using differential thermal analysis (DTA) or differential scanning calorimetry (DSC). Maximum temperatures for these instruments are about 1,700°C. At this temperature, many of the important

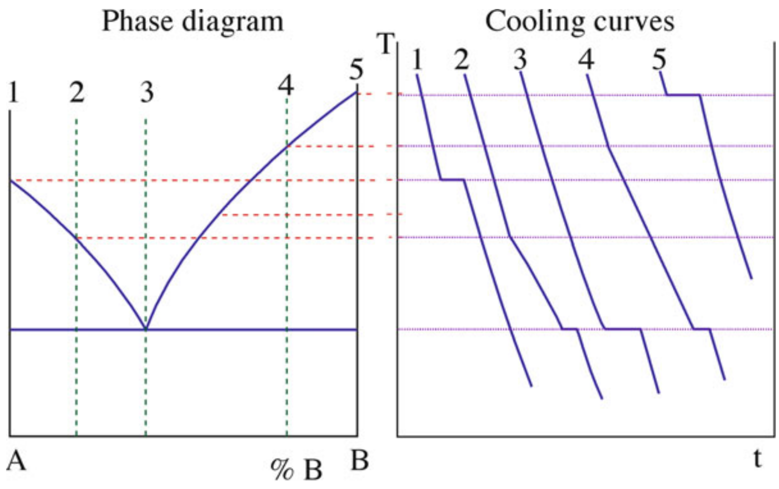

FIGURE 8.1. The use of cooling curves for determining the liquidus and eutectic in a binary phase diagram.

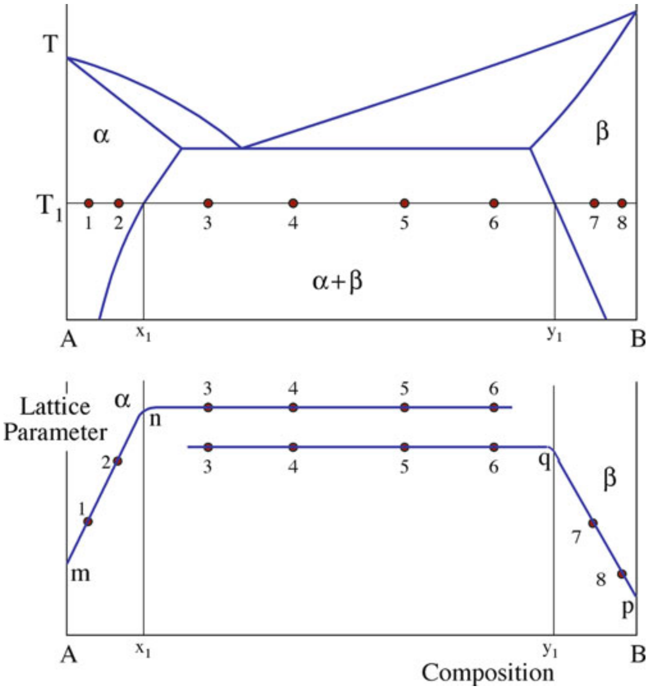

FIGURE 8.2. Parametric method for determining the solvus lines in a binary phase diagram.

ceramics such as Al_2O_3 (melts at 2,054°C), SiO_2 (melts at 1,710°C), and ZrO_2 (melts at 2,677°C) are still solid. Another problem with ceramic melts, especially those containing SiO_2, is their high viscosity. Most oxide glasses are silicates. Crystallization from these melts is often difficult, and reaching equilibrium can take a very long time (years!).

A frequently used method for studying phase equilibria in ceramics is X-ray diffraction on samples that have been equilibrated at high temperature and then quenched. This technique is particularly useful for the solid-state portions of the phase diagram, such as determining the position of the solvus lines. In each single solid solution region of a binary phase diagram there is a change in lattice parameter with composition. In the phase field where both solid solutions exist, the lattice parameter of each solid solution remains constant, with composition as shown in Figure 8.2. The position of the solvus line, at a particular temperature, corresponds to the change in slope. It is important that the conditions are sufficient for the system to reach equilibrium and that high-purity powders are used.

We can calculate phase diagrams using the requirement that the lowest free energy state is the equilibrium one. If calculations are performed for a range of temperatures, then the phase boundaries can be determined. Because we often don't know the absolute values for thermodynamic quantities, but changes in these, we use the expression:

$$\Delta G = \Delta H - T\Delta S \tag{8.1}$$

ΔH and ΔS can be determined at any temperature using the heat capacity, c_p

$$\Delta H_{T_2} - \Delta H_{T_1} = \int_{T_1}^{T_2} \Delta c_p dT \tag{8.2}$$

and

$$\Delta S_{T_2} - \Delta S_{T_1} = \int_{T_1}^{T_2} \frac{\Delta c_p}{T} dT \tag{8.3}$$

The problem is that heat capacities are not known for many compounds. As a result, we often make assumptions that allow us to determine a part of the phase diagram that is important to us.

8.2.1 Estimation of Liquidus and Eutectic Temperature for a Binary System

We can estimate the position of the liquidus assuming that our mixture forms an ideal solution; hence it obeys Raoult's law. From the Clausius-Clapeyron equation with some integration and algebraic manipulation we can obtain

$$\ln X_A = -\frac{\Delta H_f}{R}\left(\frac{T_M - T}{T_M T}\right) \tag{8.4}$$

where X_A is the mole fraction of component A and ΔH_f is the enthalpy of fusion. Values of T are plotted against composition. At the intersection of these lines is the eutectic point. This approach works well for many alkali halide systems (e.g., the NaF–KF system) but not so well for many oxides. For example, the PbO–B_2O_3 system shows dissociation on melting.

An alternative method for calculating the liquidus is to calculate differences in free energy of the solid (G_s) and liquid (G_l) phases as a function of temperature.

CLAUSIUS-CLAPEYRON EQUATION

Change in vapor pressure (P) of a solid with a change in T

$$\frac{dP}{dT} = \frac{\Delta H_S}{T(V_V - V_S)}$$

ΔH_S = enthalpy of sublimation of solid
V_V = molar volume of vapor
V_S = molar volume of solid

SOME USEFUL DATA

NiO $T_M = 2{,}257$ K; $\Delta H_f = 50.6$ kJ/mol
MgO $T_M = 3{,}073$ K; $\Delta H_f = 77.4$ kJ/mol
BeO $T_M = 2{,}830$ K; $\Delta H_f = 71.1$ kJ/mol
UO_2 $T_M = 3{,}150$ K; $\Delta H_f = 54.0$ kJ/mol

$$G_s - G_l = -\Delta H_f \ln \frac{T_M}{T} \qquad (8.5)$$

We need to know the enthalpy of fusion, ΔH_f and the melting temperature, T_M.

Figure 8.3 shows how this method has been used to construct the phase diagram for the UO_2–BeO system. The agreement with the published diagram is quite good.

8.2.2 Estimation of Liquidus and Solidus for Systems with Complete Solid Solubility

Figure 8.4 shows free energy versus composition plots at 2,700°C for the NiO–MgO system and the corresponding phase diagram. This system is one where the components are mutually soluble in both the solid and liquid states. Determination of the free energy curves uses equation 8.5 and the free energy change associated with mixing liquid NiO and liquid MgO, which can be calculated using

$$\Delta G = RT[X \ln X + (1 - X)\ln(1 - X)] \qquad (8.6)$$

The use of computer methods for calculating phase diagrams is becoming increasingly important. The results of many of these studies are available in CALPHAD: Computer Coupling of Phase Diagrams and Thermochemistry (Saunders 1998 and online). Figure 8.5 illustrates such computed phase diagrams.

8.3 PHASE DIAGRAMS FOR CERAMISTS: THE BOOKS

The books are really important for ceramics, so we emphasize them here rather than just at the end of the chapter. All ceramicists must be familiar with “the books.” The first volume of the series “Phase Diagrams for Ceramists” was published in 1964 and is in daily use. The series currently contains 12 volumes. The companion volume by Bergeron and Risbud is entitled *Introduction to Phase Equilibria in Ceramics* and should always sit on the same shelf. The books are unique in that the later volumes contain both new and updated diagrams, but the old diagrams found in the

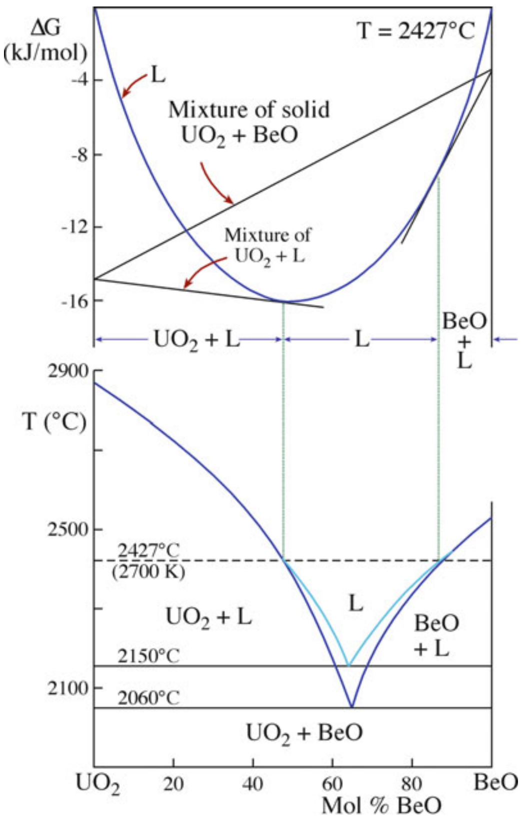

FIGURE 8.3. UO_2–BeO phase diagram determined using free energy calculations.

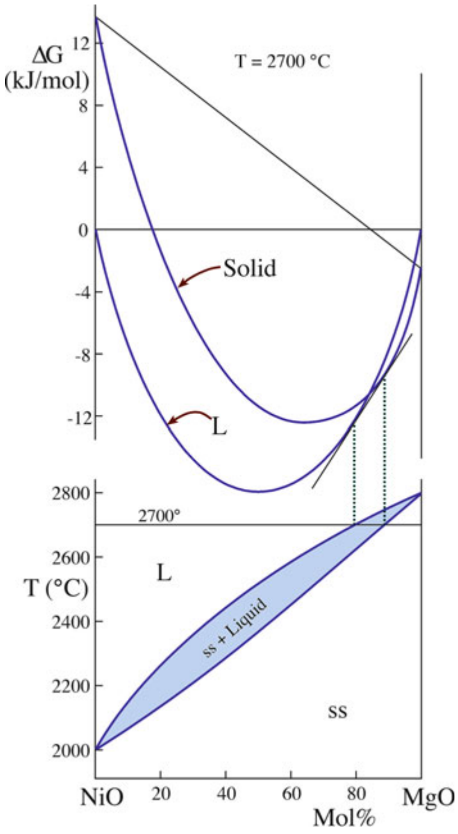

FIGURE 8.4. NiO–MgO phase diagram and free energy curves at $T = 2{,}700°C$.

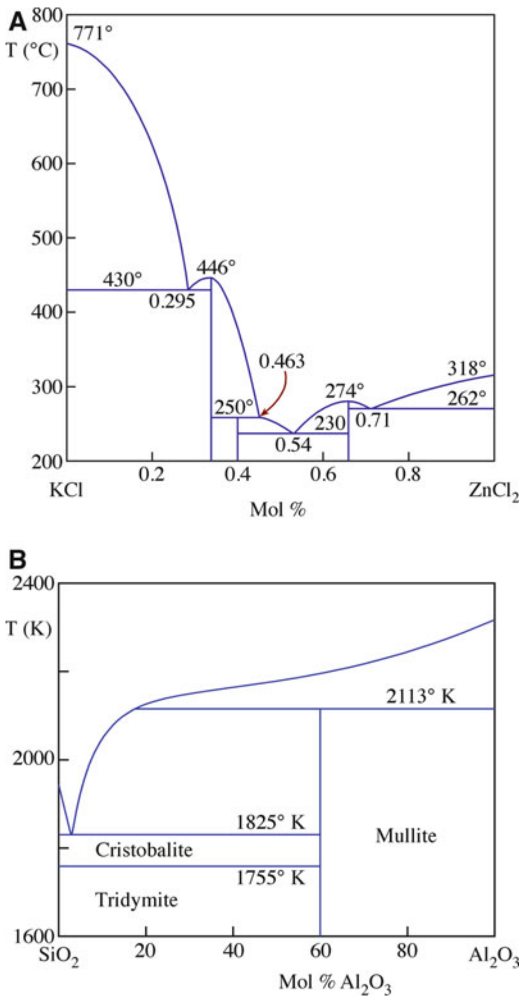

FIGURE 8.5. (a) CALPHAD phase diagram for KCl–$ZnCl_2$. (b) CALPHAD phase diagram for SiO_2–Al_2O_3.

earlier volumes are still often quoted. Many of these diagrams resulted from research in the 1950s and 1960s, but there are many going back to 1915. The first diagram in the book (Figure 1) was produced in 1951 and is for the system Al–Al_2O_3. It shows the gaseous species over liquid Al_2O_3 as a function of T and P. One of the earliest is for the $AgNO_3$–$NaNO_3$ system, which was devised in 1900 (Figure 1040). Unfortunately, this field is not currently well supported. In our brief discussion in this chapter, we take the approach of "learn by example."

A warning on units is necessary. As many of the data were collected before the establishment of SI units, the plots contain combinations of weight percent, mole fraction, and mole %; kbars and atm for pressure; but fortunately only °C (not °F) for temperature.

GIBBS C, F, AND X

C for component
F for freedom
X for phase

8.4 GIBBS PHASE RULE

We derive the Gibbs Phase Rule in three steps.

Step 1. Consider the situation where we have C components that exist in X phases. If Fe and O are the components, Fe and FeO would be examples of phases. Thus, there are XC composition variables. Adding the two important external variables in ceramics, P (pressure) and T, gives $XC + 2$ variables.

Start with $XC + 2$

Step 2. If we described the composition of a phase in terms of the mole fraction of its components, then when we have described all but one of the mole fractions; the last one must be known because together the mole fractions all add up to unity. This happens for each of the X phases, so X of the variables are actually fixed.

Deduct X

Step 3. In equilibrium, the chemical potential of a component must be the same in all the phases (otherwise it won't be equilibrium). If the concentration is fixed in one phase, then the chemical potential is fixed in that phase. The chemical potential must then be fixed in all the phases because it's the same in all phases. Thus, if the concentration is known in one phase, then $X-1$ variables (the concentrations in the other phases) are automatically fixed (even though they are not necessarily the same, their chemical potential is the same). Because this is true for all C of the components, $(X-1)C$ variables are fixed (they are not independent variables).

Deduct $(X-1)C$

Hence the number of independent variables is given by

$$F = (XC + 2) - X - (X - 1)C$$

Rearranging gives us Gibbs Phase Rule.

$$F + X = C + 2 \tag{8.7}$$

Note that many texts use P for the number of phases and V for the degree of freedom. We use F for (degrees of) freedom. Our P is an important variable—the pressure; and V is our volume. We use X for the number of phases.

Most of the time we just examine different systems with up to three components ($C = 1$, 2, or 3). The

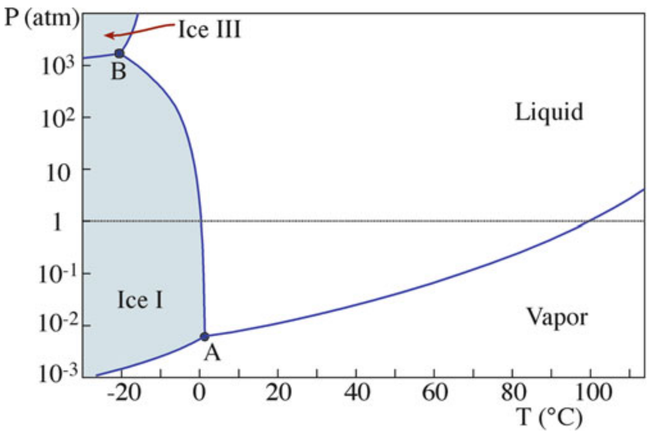

FIGURE 8.6. H_2O phase diagram (1,000 atm. is ~100 MPa).

difficulty sometimes is in counting the components. There are also four and five component diagrams in ceramics. We always have to be aware that the sample might contain nonequilibrium phases.

8.5 ONE COMPONENT (C = 1)

In each of these examples, we have one component, meaning that the chemical composition of the material does not vary. From the phase rule, we have P and T as two variables, which is what we plot in each case. Using $F + X = C + 2$ for a one-phase region, we can vary both P and T. For a two-phase region (the line), if we vary P then T is determined. For a three-phase region in a one-component system there are no variables.

Example 1 Water: one component (Figure 8.6). X takes its maximum value of three when $F = 0$. The three coexisting phases are then solid, liquid, and gas at point A, or the liquid and two solid phases at point D. Points A and D occur at unique combinations of temperature and pressure. Lines correspond to locations where two phases are in equilibrium ($X = 2$ and $F = 1$). If we vary T, then P must vary so we stay on the line. This diagram is a simplification of what we know now because there are many (11 or 12) other known crystalline forms of ice. The form that occurs in nature is called ice Ih (a hexagonal form) and has a density of 0.931 g/cm^3 (water is 1.00 g/cm^3; hence the iceberg phenomenon). The other forms exist at either lower values of T or higher values of P than shown in Figure 8.6. (We've kept this pressure in atmospheres because the most important equilibrium occurs at 1 atm).

Example 2 Carbon: one component (Figure 8.7). This is a classic example of an element with three solid phases. We often remind owners that diamonds are only metastable, but fortunately the kinetics of the phase transformation are very slow. Notice where we live—in a dot at the bottom left corner.

Example 3 SiO_2: one component (Figure 8.8). Silica is not only one of the most important ceramics but its phase diagram is also very interesting. Remember, the composition is constant. This schematic diagram emphasizes both the relationship between the glass and the liquid and the fact that the glass is the high-pressure phase; the glass is denser than any of the crystalline forms (similar to ice). The phase rules always apply.

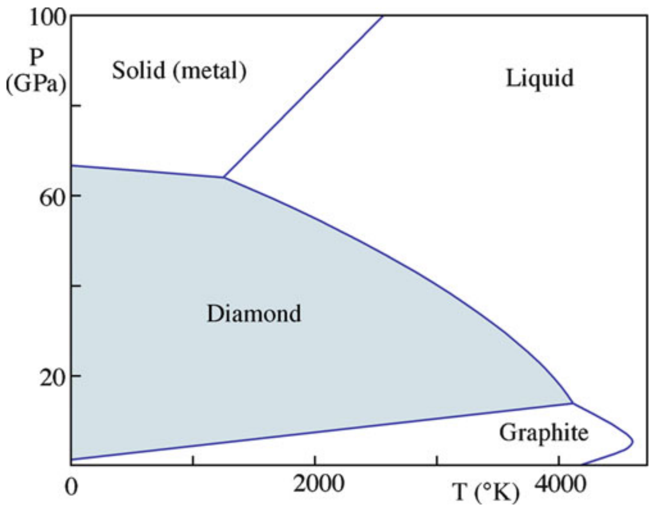

FIGURE 8.7. C phase diagram.

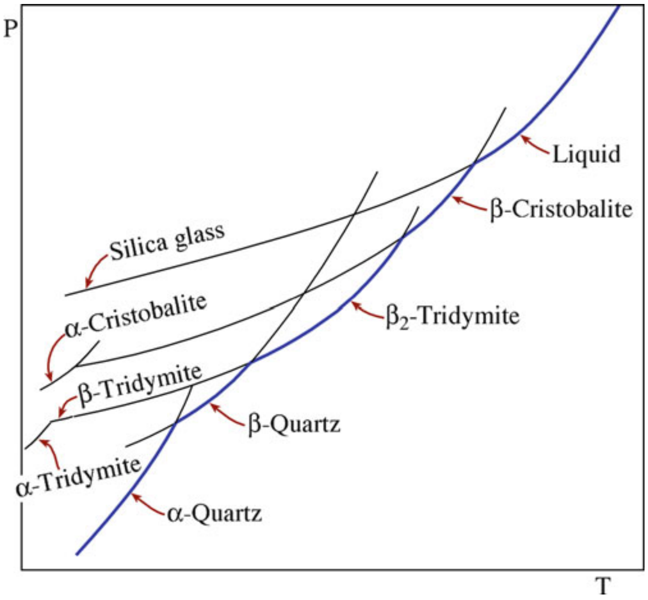

FIGURE 8.8. SiO_2 phase diagram.

8.6 TWO COMPONENTS (C = 2)

Binary phase diagrams are very important for ceramics. The two most important cases for ceramics are the combination of a metal plus oxygen and the combination of two oxides. A model two-component system is shown in Figure 8.9, where you can see we are now using the third dimension to display the data.

If there is one phase ($X = 1$), as at B, then the three variables are pressure, temperature, and one other—for example, the composition (x/y ratio).

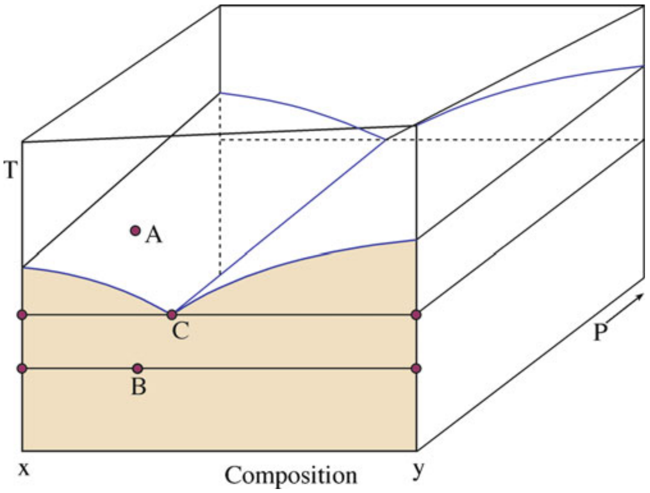

FIGURE 8.9. Model binary phase diagram showing *T*, *P*, and composition as variables.

If there are two phases present ($X = 2$), such as the liquid and one solid phase at A, then $F = 2$. If, for example, we fix P, we are free to vary T and move along the liquid/solid phase boundary (a surface).

The special feature is that we have introduced surfaces into the phase diagram. In ceramic materials, the gas phase may be very important. This is where ceramics are particularly different from metals: oxygen (or nitrogen or water vapor and hence hydrogen) may be a component of the system. The gas phase is not important if the valence of the cations is fixed and the total pressure, P, is fixed at 1 atm. We consider materials with variable valence in Section 8.8.

Example 1 NiO/CoO: Two components and P fixed (Figure 8.10). The special feature about this diagram is that both oxides have the rock salt structure. Pauling's rules tell us not to be surprised that they are fully interchangeable. However, it's reported that there is a two-phase region at low temperatures. Notice three points:

- At the high temperatures, the diagram contains only dashed lines—intelligent guesses.
- The two-phase region occurs where kinetics are quite slow.
- The composition is given as a mole fraction.

This is a case where you start with "the book" and then go back to the original reference to learn how the pO_2 was controlled, how the two phases were identified, and so on.

Example 2 MgO/CaO: Two components and P fixed (Figure 8.11). This diagram is a classic eutectic even though CaO and MgO both adopt the rock salt structure. Because the sizes of the two cations differ by more than 15%, solid solubility is limited.

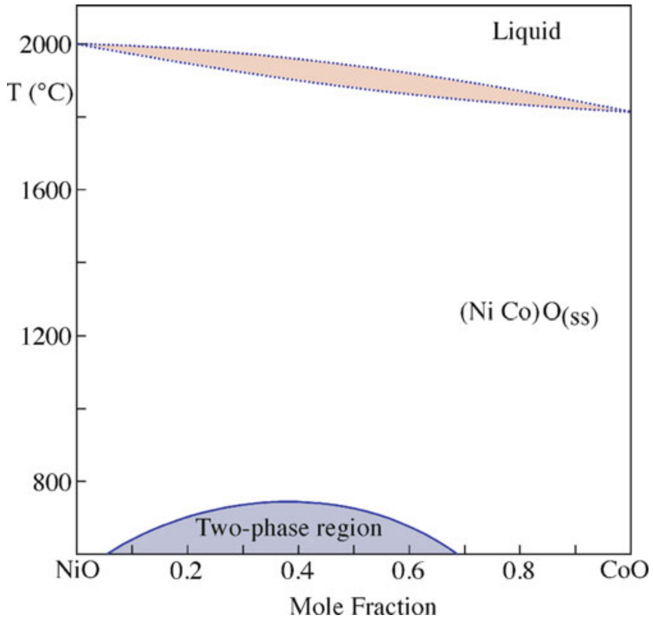

FIGURE 8.10. NiO–CoO phase diagram.

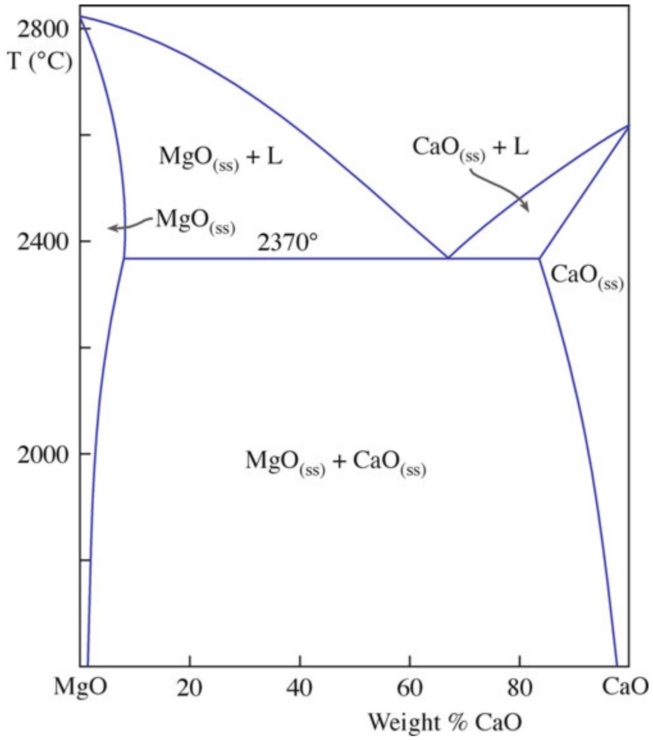

FIGURE 8.11. The MgO–CaO phase diagram.

Example 3 $MgO/MgAl_2O_4/Al_2O_3$: Two components and P fixed (Figure 8.12). This is a particularly important, but relatively simple, system in ceramics. It involves three widely used materials, which are also archetypical structures. We can choose the two components to be MgO and Al_2O_3. Then, in the one-phase region we have two variables in addition to P and T. In the two-phase region (along the boundaries) we can vary T and the Mg: Al ratio. Notice that the composition is given in weight percent, which is not too bad for this system but really

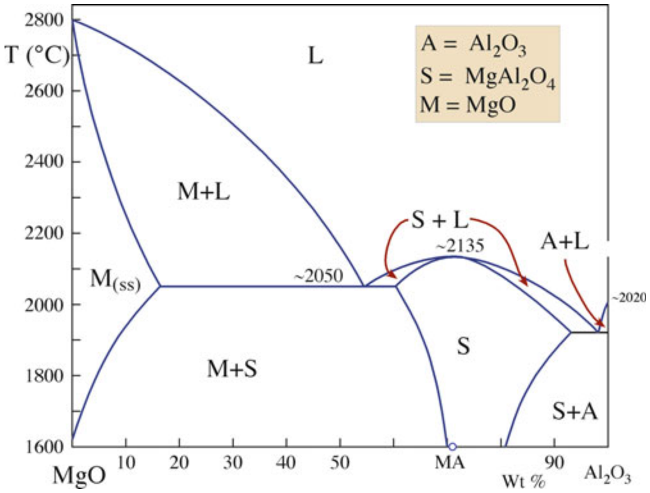

FIGURE 8.12. MgO–Al_2O_3 phase diagram.

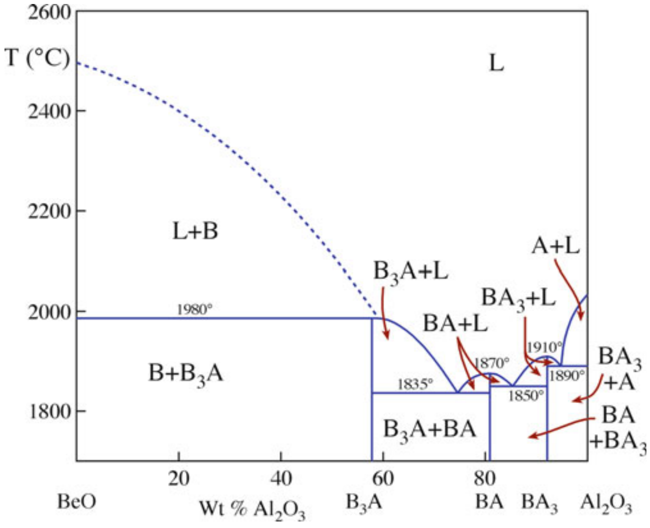

FIGURE 8.13. BeO–Al_2O_3 phase diagram.

distorts the related MgO/Cr_2O_3 and NiO/Al_2O_3 systems. The spinel phase field is already quite wide at 1,600°C and becomes wider at high temperatures, especially toward the Al_2O_3-rich side. We can grow two eutectic structures; one essentially contains pure Al_2O_3.

Example 4 BeO/Al_2O_3: Two components and P fixed (Figure 8.13). Notice that all the phases can be regarded as combinations of BeO and Al_2O_3, so we can denote them as B_3A, BA, and BA_3. From the chemical point of view, the system looks quite similar to MgO/Al_2O_3, but clearly it is very different: three separate eutectics are shown; and none of the compounds has the spinel structure. $BeAl_2O_4$ is the mineral chrysoberyl and has a structure similar to olivine, which is not unrelated to spinel.

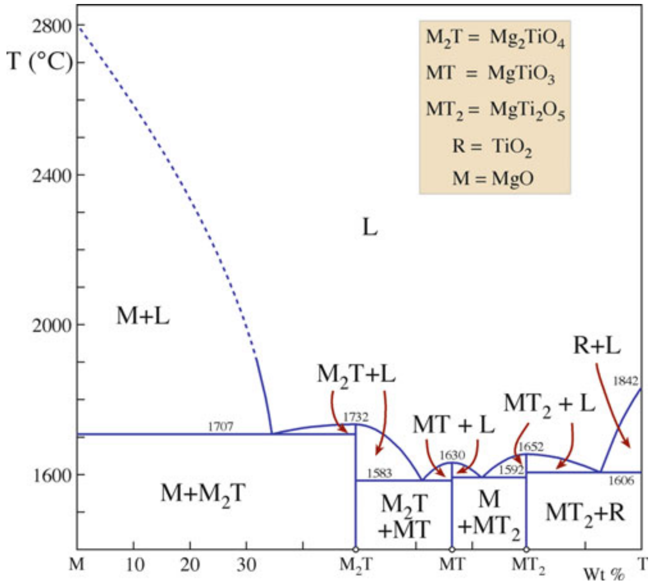

FIGURE 8.14. MgO–TiO_2 phase diagram.

Example 5 MgO/TiO_2: Two components and P fixed (Figure 8.14). This system is interesting because of the occurrence of four different eutectics. Such eutectics in this and other systems have been used to prepare some interesting two-phase materials. For example, when a liquid with composition in the MgO-rich region is cooled from the eutectic temperature at 1,707°C, it produces a material that consists of alternating lamellae of nearly pure MgO and Mg_2TiO_4. Other systems show different structures, which are determined in part by the interfacial energies. Of course, interfacial energies are usually not considered in the analysis of phase diagrams.

HUME-ROTHERY RULES FOR COMPLETE SOLID SOLUBILITY

- Same crystal structure
- Equal valence
- Ionic radius within ±15%
- No chemical reactivity

If we have two oxides we need only consider the sizes and valences of the cations.

8.7 THREE AND MORE COMPONENTS

When three components (ternary systems; $C = 3$) are present, the phase diagrams become more difficult to draw because we then have $F + X = 5$. If the pressure is fixed, then we have four variables. We need one axis for each component and one for the temperature, for example, so we draw the compositions on a triangle and plot T as the vertical coordinate, as shown in Figure 8.15A. The base triangle is called the Gibbs triangle. The example shown in Figure 8.15A corresponds to the case where three oxides form solid solutions (extending the NiO/CoO example).

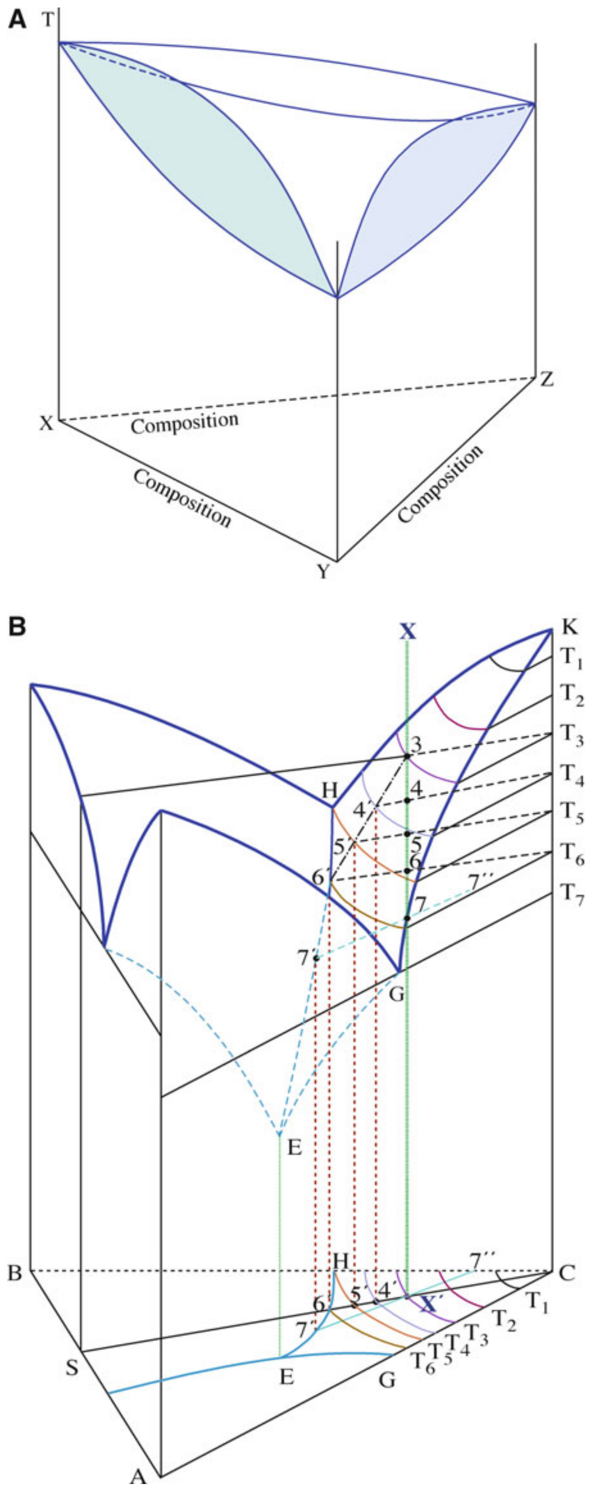

FIGURE 8.15. (A) A model ternary phase diagram for a system showing three solid solutions. (B) A model ternary phase diagram for a system showing three eutectics.

The example shown in Figure 8.15B is the case of three simple binaries, each with a single eutectic (extending the MgO/CaO example). Figure 8.15B is worth some effort to understand. The lines of constant temperature at the solid/liquid phase boundary are projected onto the base of the Gibbs triangle. The location of each of the three eutectics is also projected and correspond to an abrupt change in the curvature of the constant-temperature contour. The three eutectics then meet at a "grand eutectic" at E. For sufficiently slow cooling, E corresponds to the ultimate eutectic temperature—below T_E the sample is solid.

In the materials that are often most important, the diagrams are more complicated. The phase diagram books then often show them as projected triangles as in Figures 8.16, 8.17, and 8.18.

Example 1 $MgO/Al_2O_3/SiO_2$: Three components and P fixed (Figure 8.16). Notice that there are perhaps three locations for E. This diagram contains several really important ceramics. We have already examined one of the binary diagrams included here (MgO/Al_2O_3) and will examine another below (MgO/SiO_2). Diagrams such as this have difficulty showing what is happening at temperatures other than the liquidus.

Example 2 $CaO/Al_2O_3/SiO_2$: Three components and P fixed (Figure 8.17). This figure illustrates the extension of the use of abbreviations to three components. It also illustrates how you can combine the eutectics with a set of tie lines. The CA_n ceramics are found in high-alumina cements. The phases are all shown as being crystalline. Notice that CS is close to the midpoint, but AS and CA are closer to Al_2O_3.

Example 3 $Na_2O/CaO/SiO_2$: Three components and P fixed (Figure 8.18). This system is particularly interesting because of its relevance to soda-lime glass formation. Because of this interest, the diagram has been limited to the silica-rich corner of the Gibbs triangle.

Each of these diagrams shows the contours of the solid/liquid boundary. It is now a little more difficult to envision what occurs as we lower the temperature of the liquid phase. The basic ideas are the same as for the two-component systems, as shown in Figure 8.19. The cooling path follows the steepest descent on the liquidus—in this case it reaches T_E—at which point the whole sample is solid and kinetics become the controlling factor.

8.8 COMPOSITION WITH VARIABLE OXYGEN PARTIAL PRESSURE

The gas phase, particularly the oxygen partial pressure, pO_2, is important when the valence of the cation can change.

In ceramics, we usually run experiments at 1 atm., but geologists are interested in much higher pressures, and hot pressing is an established commercial method for processing ceramics.

There are two ways to control the pO_2. Usually, we don't try to change or control the total pressure—we avoid

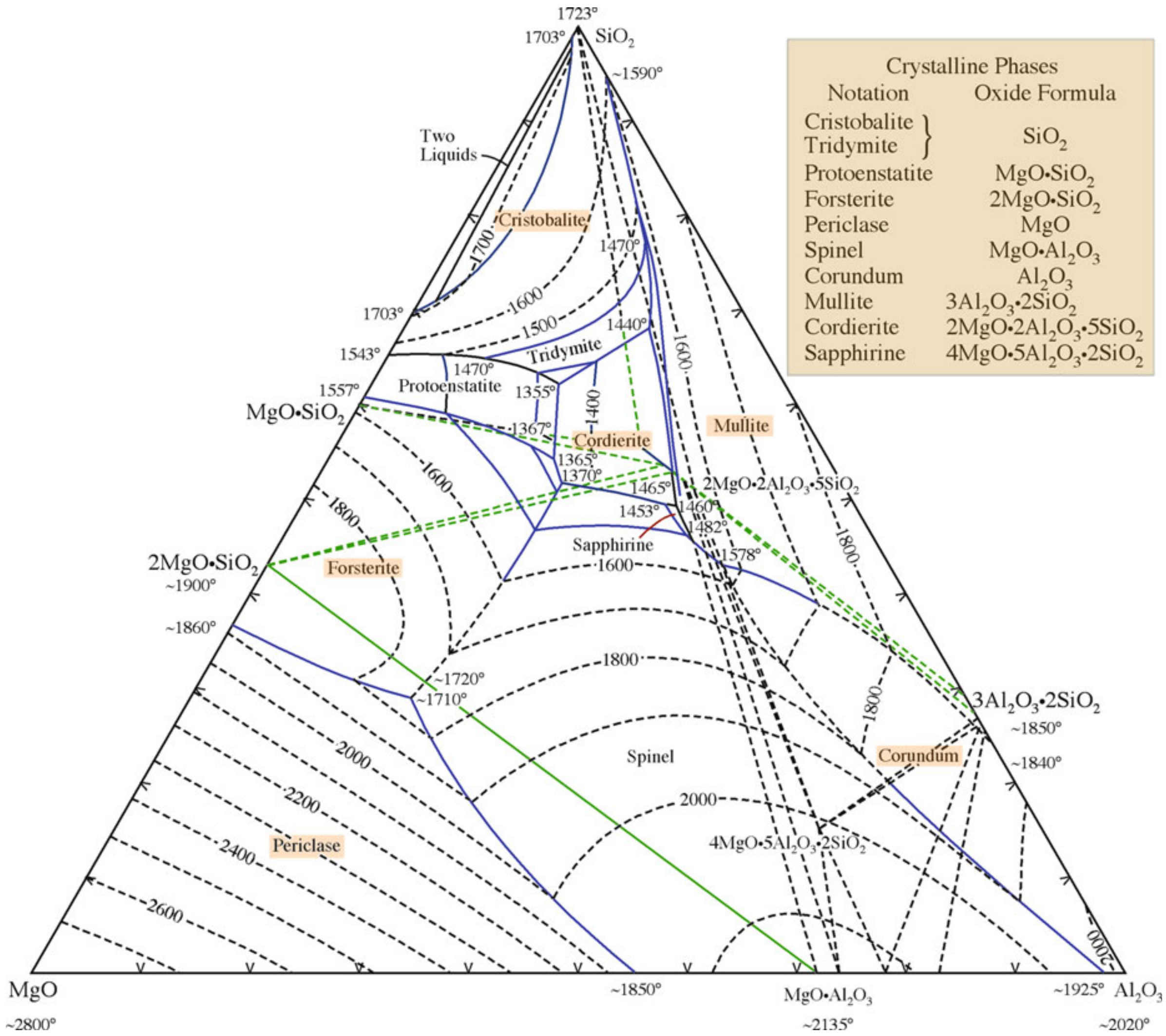

Crystalline Phases

Notation	Oxide Formula
Cristobalite Tridymite	SiO$_2$
Protoenstatite	MgO•SiO$_2$
Forsterite	2MgO•SiO$_2$
Periclase	MgO
Spinel	MgO•Al$_2$O$_3$
Corundum	Al$_2$O$_3$
Mullite	3Al$_2$O$_3$•2SiO$_2$
Cordierite	2MgO•2Al$_2$O$_3$•5SiO$_2$
Sapphirine	4MgO•5Al$_2$O$_3$•2SiO$_2$

FIGURE 8.16. The MgO–Al$_2$O$_3$–SiO$_2$ phase diagram.

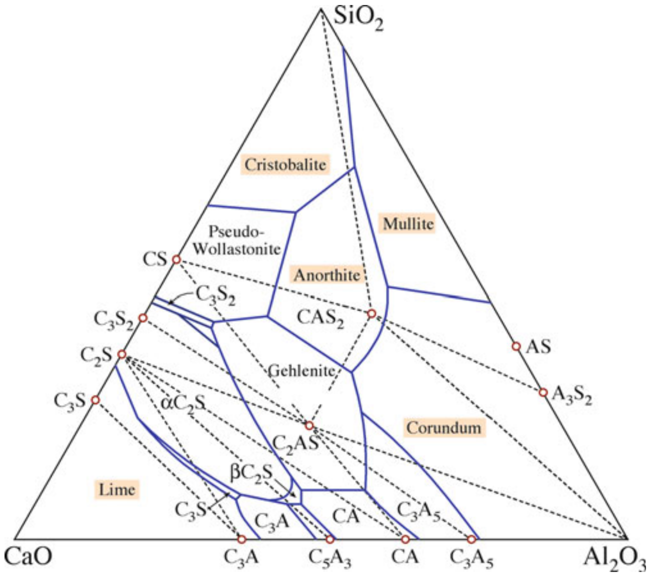

FIGURE 8.17. CaO–SiO$_2$–Al$_2$O$_3$ phase diagram.

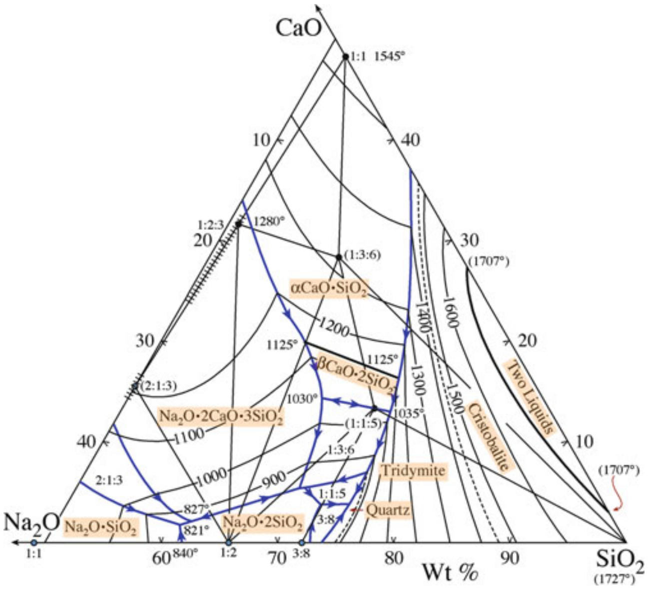

FIGURE 8.18. Na$_2$O–CaO–SiO$_2$ phase diagram.

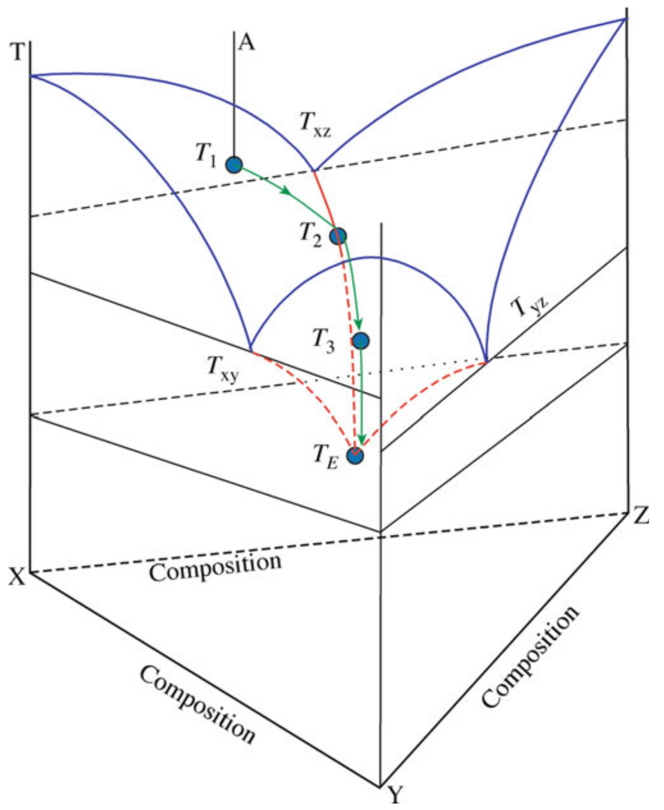

FIGURE 8.19. Cooling path in a ternary system.

vacuum systems whenever possible because they greatly increase the expense. The approach used is to fix the pO_2 using one of the following reactions

$$CO + \frac{1}{2}O_2 = CO_2 \tag{8.8}$$

$$H_2 + \frac{1}{2}O_2 = H_2O \tag{8.9}$$

If there is no solid present, then we have just one phase; namely, the gas and $X + F = C + 2$ gives $F = 3$. So we can vary T, P_{total} and the composition (CO_2/CO ratio or H_2/H_2O ratio).

If there is a solid present (e.g., graphite or Ni), then we have just two variables (because we have two phases, $X = 2$), which fixes the system. If Ni is present, for example, then essentially the Ni/NiO equilibrium sets the pO_2. The same occurs if Fe is present.

We spend some time now discussing the Fe-O diagram shown in Figure 8.20. Here, gas is important. In the Fe–O phase diagram, we have two components. We can call them Fe and O or FeO and Fe_2O_3 as we wish. The special feature in Figure 8.20 is the fact that usually the lines of constant pO_2 are horizontal, whereas in two-phase fields they are inclined to the horizontal. They are inclined when the phase field contains a single phase (wüstite or magnetite).

In the two condensed phases region (*region W+M*): There are two condensed phases plus the gas (O_2), so $X = 3$. There are two components ($C = 2$; Fe and O), so we have only one degree of freedom: we can vary T or pO_2. Therefore, the oxygen isobars (lines of constant pO_2) on the phase diagram must be horizontal.

In the wüstite phase (*region W*): There is one condensed phase plus the gas (O_2), so $X = 2$. There are two components ($C = 2$; Fe and O), so we have 2° of freedom ($F = 2$). The reason the isobars have the particular slope is that they must connect the appropriate isobars at each side of their phase field.

This is the special feature for ceramics, especially when processing ceramics with a variable-valence cation in air: pO_2 is important.

Figure 8.20A shows the Fe–O diagram as a function of oxygen activity, which is essentially the pO_2. This diagram shows what condensed phase is stable at each combination of temperature and pO_2. Although this diagram does not give as much information as Figure 8.19 (because it doesn't show the composition of the condensed phase), it does emphasize one special feature: if we increase the temperature while keeping the pO_2 constant, the oxidation state of the Fe ion decreases. In this figure, the areas show situations where only one phase is present, and all of the lines represent two-phase regions. If we look back at Figure 8.19, the areas represented conditions where one or two phases are in equilibrium with a gas phase.

Figure 8.20B and C shows the related diagrams for the H–O and C–O systems. These diagrams can be very useful in the laboratory because this is how we try to reach the pressures indicated in Figure 8.19A: notice that neither system easily takes us below 10^{-23} atm. In each case, the temperature is plotted against a gas partial-pressure ratio, with the curves showing the contours for constant pO_2. The curves are for the situation where the total pressure is fixed at 1 atm, so we don't need a vacuum system. The gray area in the C–O system is instructive—we can't reach this in equilibrium because then carbon would form and the solid curve would represent equilibrium. In the gas phase, we have two components ($C = 2$) but only one phase (the gas), so $F = 3$. We can

PRESSURE CONVERSION

$1\ \text{Pa} = 1\ \text{N/m}^2 = 1\ \text{m}^{-1}\cdot\text{kg}\cdot\text{s}^{-2}$
$1\ \text{N} = 1\ \text{m}\cdot\text{kg}\cdot\text{s}^{-2}$
1 bar = 0.1 MPa
1 kbar = 100 MPa
1 atm = 1.013 Pa
1 mmHg = 1 Torr = 0.1333 MPa

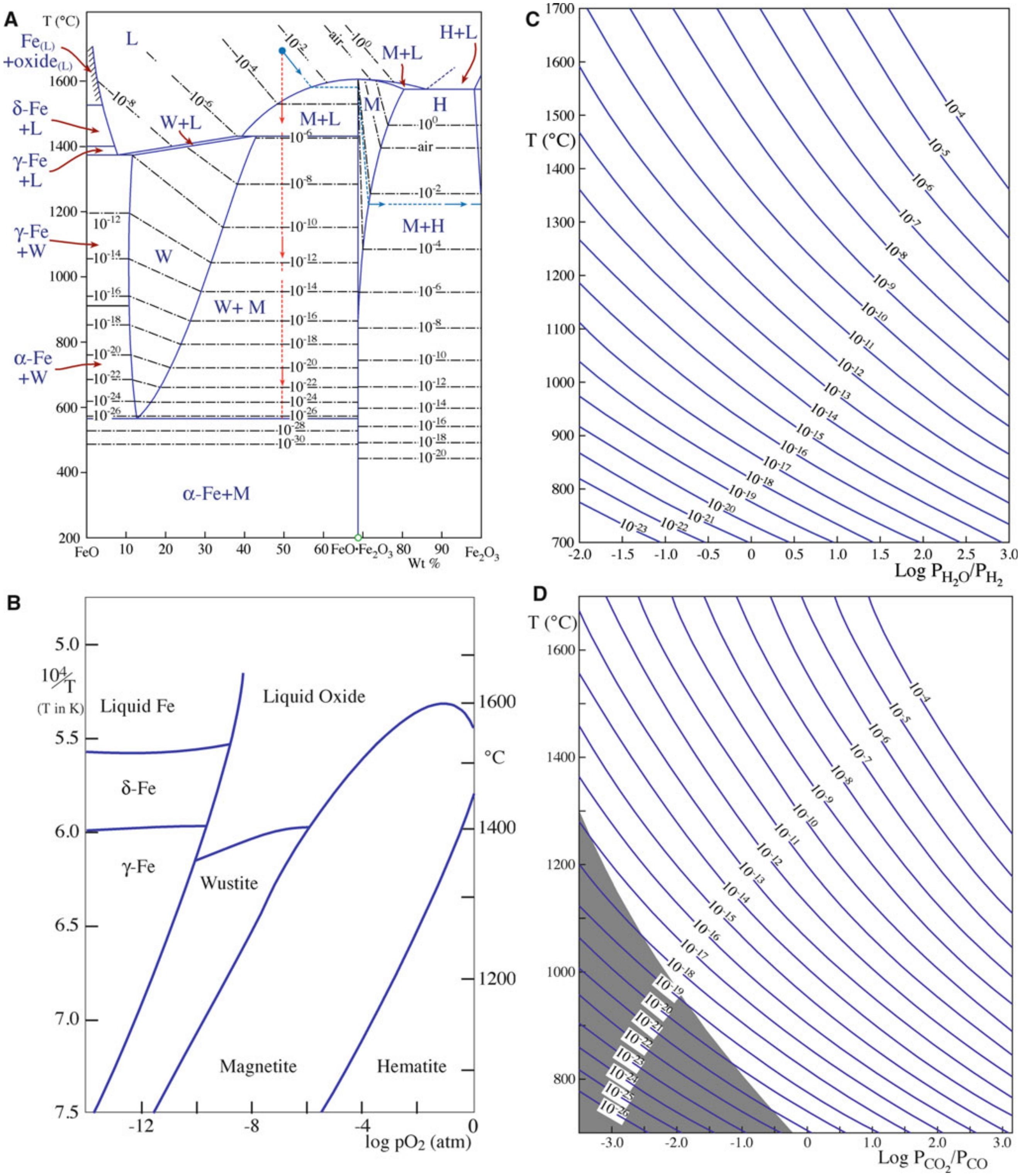

FIGURE 8.20. (a, b) The FeO–Fe_2O_3 phase diagram; (c) the H–O system; (d) the C–O system.

fix T and the total pressure and still vary pCO, $p$$CO_2$, $p$$O_2$, or a ratio of any two. If we precipitate out carbon, then we have two phases (gas plus carbon), and $F = 2$. If we fix T and the total pressure (or any of the partial pressures), there is no remaining variable.

8.9 QUATERNARY DIAGRAMS AND TEMPERATURE

The diagrams are now becoming really difficult! Figure 8.21 illustrates an Si–Al–N–O tetrahedron that clearly has difficulty showing temperature effects.

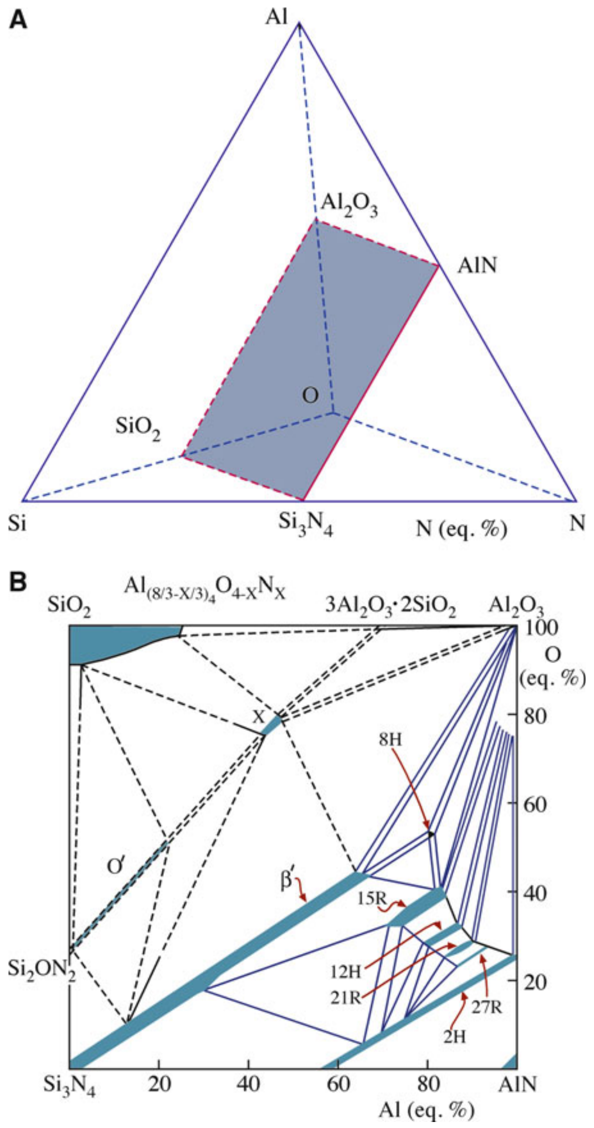

FIGURE 8.21. (a) The Si–Al–N–O phase diagram represented as a tetrahedron. (b) The Si_3N_4–SiO_2–Al_2O_3– AlN phase diagram.

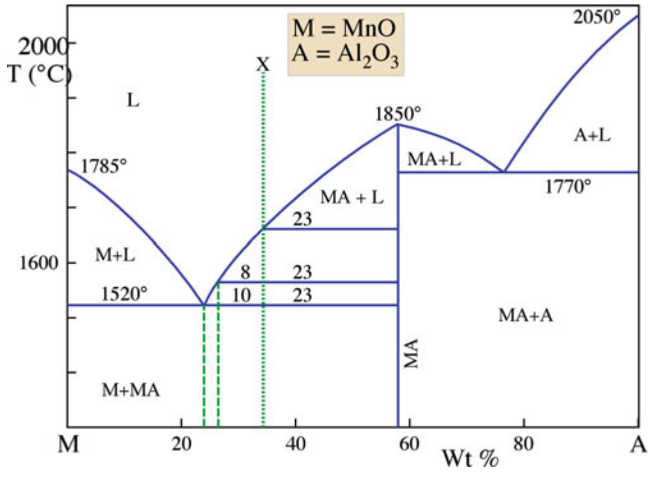

FIGURE 8.22. MnO–Al_2O_3 phase diagram.

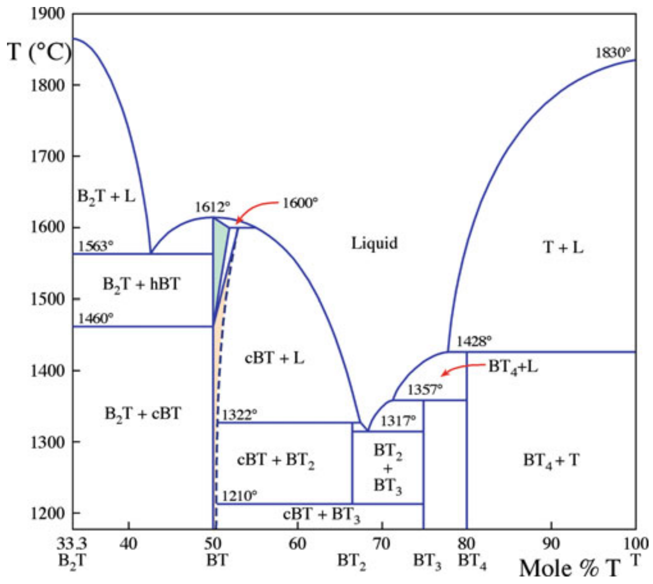

FIGURE 8.23. $BaTiO_3$ phase diagram.

The rectangle cut from it represents the SiO_2–Al_2O_3–AlN–Si_3N_4 quaternary system. Now we can plot the different true quaternary compounds, as shown in Figure 8.21B. The ceramics located in this system are then known collectively as the SiAlONs. We discussed the structures of these compounds in Chapter 7.

Notice the use of the Ramsdell notation. This example is more complicated than in Section 6.13 because the chemistry is also changing.

GIBBS FREE ENERGY OF MIXING

For an ideal solution ΔG_M is

$$\Delta G_M = RT(X_A \ln X_A + X_B \ln X_B)$$

and $\Delta H_M = 0$.
For non-ideal solutions, $\Delta H_M \neq 0$

8.10 CONGRUENT AND INCONGRUENT MELTING

Figure 8.22 shows the MnO–Al_2O_3 phase diagram. The equimolar composition melts congruently; that is, there is a direct transformation between the solid and liquid states without a change in the number of phases (in this case $X = 1$). BaO–TiO_2 is another example of a two-component system (Figure 8.23). This diagram illustrates the concept of incongruent melting: there are actually three incongruently melting compounds. The diagram also shows that we cannot produce pure cubic $BaTiO_3$ by solidifying a liquid of that composition, which is important when we discuss crystal growth later. Notice that all the compounds on this phase diagram are BT_n (BT, BT_4, etc.).

8.11 MISCIBILITY GAPS IN GLASS

Can glass be described by equilibrium phase diagrams? This question refers to the fact that glass is not itself in equilibrium. We can, however, describe some aspects of glass microstructure in terms of phase diagrams, especially that of liquid immiscibility, which leads to the phenomenon of phase separation, as illustrated in Figure 8.24.

The random-network model considers glasses as homogeneous. However, microscopic features on the scale of 3 nm to hundreds of nanometers can exist. These small features exist in a range of glasses and can result from a process of phase separation, in which a liquid that is homogeneous at high temperatures separates into two of more liquid phases on cooling.

Figure 8.25 shows the phase diagram for the $BaO–SiO_2$ system, which exhibits phase separation. The dome, shown by dashed lines because the system is metastable, is the key feature in a phase diagram where phase separation occurs (a similar dome occurs for Al_2O_3/Cr_2O_3, so this dome is not peculiar to glass).

The microstructure of glasses in the system $BaO–SiO_2$ can be determined using transmission electron microscopy (TEM). What we find is:

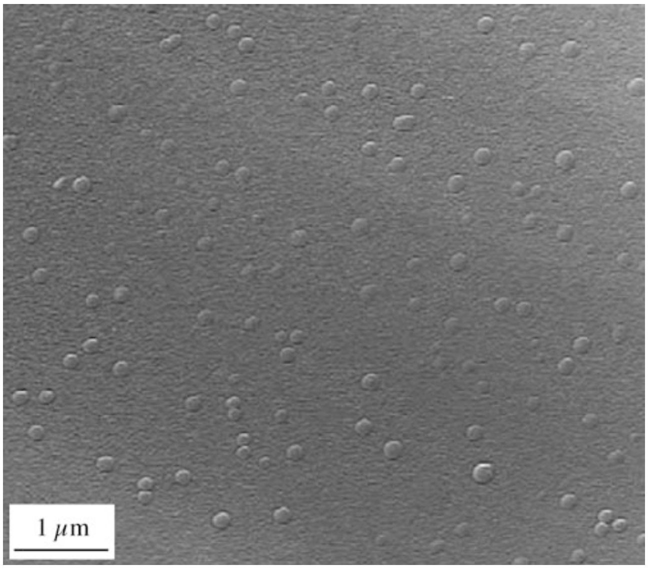

FIGURE 8.24. Image of small droplets of glass in a glass matrix. The composition of the glass is 16 wt.% CaO, 10 wt.% MgO, 14 wt.% Al_2O_3, 60 wt.% SiO_2.

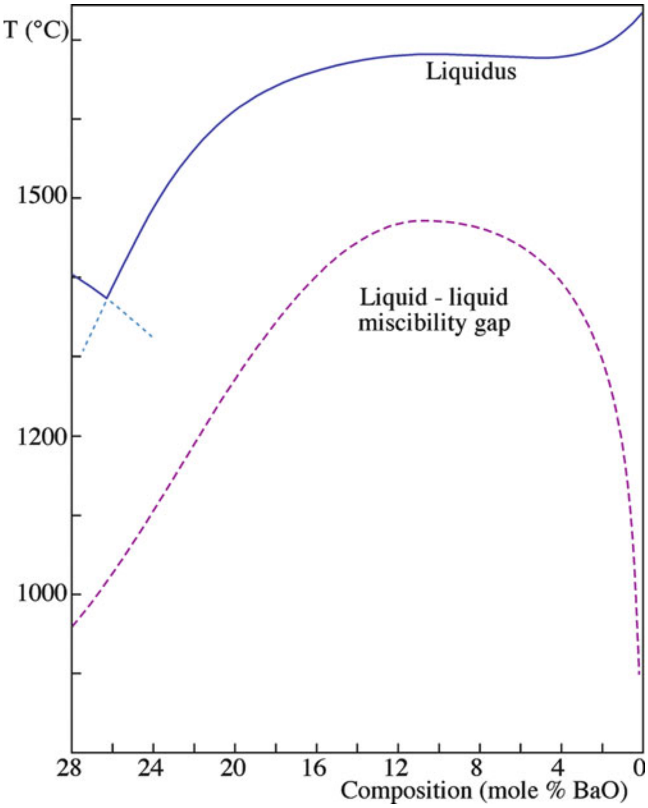

FIGURE 8.25. Silica-rich end of the $BaO-SiO_2$ phase diagram.

- At the silica-rich side of the miscibility gap there are discrete spherical particles of a BaO-rich phase embedded in a continuous matrix of an SiO_2-rich phase.
- Near the center of the miscibility gap there is a three-dimensionally interconnected mixture of BaO and SiO_2 phases.
- At the BaO-rich side of the miscibility gap there are discrete spherical particles of a SiO_2-rich phase embedded in a continuous matrix of a BaO-rich phase.

The $B_2O_3–PbO$ system is another glass-forming system that shows a miscibility gap and phase separation.

The reason for phase separation of a liquid into two phases may be found by considering the thermodynamics of mixing. Figure 8.26 shows the three thermodynamic functions, ΔG, ΔH, and ΔS plotted at temperature T as a function of composition.

The common tangent to the minima in the free-energy curve determines the composition of the two phases in the glass, and the proportions of each are determined by the lever rule.

Phase separation is important for some commercial glass formulations.

Vycor Process. Glass containing 75 wt.% SiO_2, 20 wt.% B_2O_3, and 5 wt.% Na_2O melts at relatively low

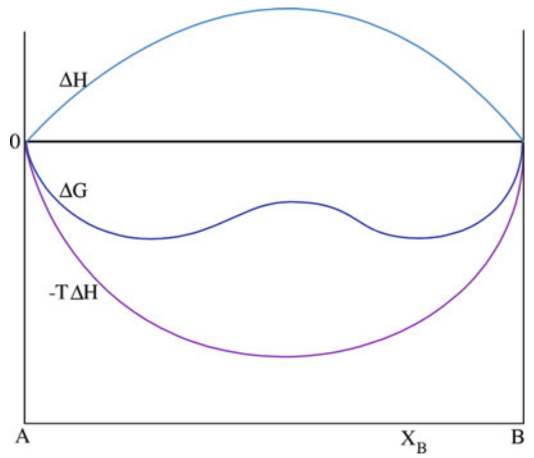

FIGURE 8.26. Energy diagram for a hypothetical system in which unmixing occurs.

temperatures due to high B_2O_3 content. It can then be formed into desired shapes and heat-treated in the range 500–600°C so the glass separates into two distinct phases, one consisting of almost pure SiO_2 and another rich in Na_2O and B_2O_3. If this product is exposed to a suitable solvent at modest temperature, the sodium borate phase is leached out, leaving a SiO_2-rich framework with a network of pores that are ~4–15 nm in diameter. This porous glass can be subsequently compacted at ~1,000°C to yield a transparent glass containing about 96 wt.% SiO_2. The advantage of this process is that we can form the silica-rich glass at relatively low temperature. It would not be feasible to shape 96% silica glass by conventional methods because of the very high temperatures required to decrease the viscosity of a high-silica glass.

Pyrex. Pyrex glass belongs to the $Na_2O–B_2O_3–SiO_2$ system also. It exhibits phase separation on a very fine scale, typically <5 nm. By controlling the cooling process, we develop a glass with a special microstructure and very useful properties. It is the inclusion of a soluble phase within an insoluble one that explains the chemical durability of Pyrex.

CHAPTER SUMMARY

Phase diagrams are key to understanding many aspects of ceramic processing. Whether we are interested in forming a material by a solid-state reaction or growing a single crystal by solidification of a melt, the first approach is to look up the appropriate phase diagram. Knowing where to find these diagrams (in the "books") is almost as important as being able to interpret them. The basic principles are the same for ceramics as they are for metals, so our approach was to highlight some important aspects of phase diagrams as they relate to ceramics.

PEOPLE AND HISTORY

We've mentioned *Boltzmann* and *Kelvin* in other chapters. Kelvin (as *William Thomson*) invented the word thermo-dynamics (now no hyphen) in 1849 when discussing Carnot's work.

Carnot, Sadi Nicolas Léonard (1796–1832) was born in Paris and was known for his engine and cycle. His book *Reflections on the Motive Power of the Fire* was published in 1824! Clapeyron discovered the work, and Kelvin and Clausius later put his theory on the correct footing.

Clapeyron, Benoît Paul Émile (1799–1864) was born in Paris and wrote the *Driving Force of Heat*. His name is closely associated with Clausius, who published *Über die bewegende Kraft der Wärme* in 1850. (See his Googlebook if your German is good.)

Clausius, Rudolf Julius Emanuel (1822–1888) was born in Köslin Germany, which is now Koszalin in Poland and gave us entropy in 1865.

Gibbs, Josiah Willard (1839–1903) was born in New Haven, Connecticut. He was educated at Yale University and was awarded his doctorate in 1863—the first doctorate of engineering to be conferred in the United States. He was appointed professor of mathematical physics in 1871 prior to having any publications. He published the first part of his very famous work *On the Equilibrium of Heterogeneous Substances* in 1876 and the second part in 1878. He published many other important papers in thermodynamics as well as in other areas of physical science.

Hume-Rothery, William (1899–1968) founded the Department of Metallurgy (now the Department of Materials) at Oxford University in the mid-1950s. H.R., as he was known at Oxford, was the author of many books on metallurgy. One of his books *Electrons, Atoms, Metals, and Alloys* is a dialogue between an older metallurgist and a younger scientist.

Le Chatelier, Henry (1850–1936) is known for his principle and for inventing the optical pyrometer in 1892

EXERCISES

8.1 The iron–iron carbide phase diagram is probably the most important of all binary phase diagrams. Why is the diagram not a true equilibrium diagram? Does it matter?

8.2 Explain what we mean by the set of equations $\mu_1{}^a = \mu_1{}^b = \ldots = \mu_1{}^c$. What is the significance of this expression?

8.3 The maximum operating temperature of high-temperature X-ray diffraction is 2,500°C in vacuum but only 1,700°C in air. Why the big difference? What, if any, effect would the lower operating temperature in air have on the determination of phase diagrams?

8.4 The UO_2–BeO system shown in Figure 8.3 does not show any solid solution formation. Would you expect it to?

8.5 With reference to the phase diagram for water (Figure 8.6), explain (a) how the boiling point of water would change if you were to climb to the top of a mountain and (b) why ice-skating is possible.

8.6 Using Figure 8.7, determine the necessary conditions for direct conversion of graphite to diamond.

8.7 Using Figure 8.8, indicate all the triple points in the SiO_2 system.

8.8 Describe fully what happens when you cool down a melt of 40 mol% NiO–60 mol% MgO. Give the compositions of the phases and their relative amounts for at least three temperatures in the two-phase field.

8.9 Describe the phases that you expect to form as a liquid of composition $BaTiO_3$ is cooled down to room temperature. Given the statement we make in Section 8.10 about the growth of single crystals of cubic $BaTiO_3$, what factors besides thermodynamics determine our ability to grow single crystals?

8.10 You have a sample containing 20 wt.% of Fe oxide in a pO_2 of 10^{-12}. What is the temperature of the sample. What happens to the sample if you slowly reduce the temperature?

8.11 Choosing a pO_2 of 10^{-12}, show how Figure 8.20A and B are related.

8.12 Consider the 10^{-12} curve in Figure 8.20C. What has this got to do with the 10^{-12} line in Figure 8.20A?

8.13 The three solid oxides in Figure 8.12 have very different phase fields. Discuss why this may be the case and what implications it may have.

8.14 Vonnegut's ice-nine is fictional even though Langmuir was reputedly the inspiration for it. What has this got to do with Figure 8.6?

8.15 CaO and MgO have the same crystal structure, but the 50:50 composition exists as two distinct phases. Explain why this is so and why we ask the question.

8.16 Explore the phase diagram in Figure 8.23 to show why we have difficulty growing crystals of $BaTiO_3$. Draw the diagram in detail.

8.17 More difficult: explore the literature to suggest why Ba_2A and BaA_2 are not found.

8.18 Apply equation 8.7 to regions W, M, and M + H in Figure 8.20A and 15R in Figure 8.21.

8.19 Imagine you have 1 g of iron oxide. What phases would you expect to have if it were in thermodynamic equilibrium? Is this what you would have expected before consulting the phase diagram? (Explain.) How might the situation change if the particles were 1-nm cubes?

8.20 Are there any examples of hot stages for TEMs that do not require a vacuum? Is the same true for SEMs?

GENERAL READING

Bergeron CG, Risbud SH (1984) Introduction to phase equilibria in ceramics. The American Ceramic Society, Westerville, This should be available in every ceramics lab
DeHoff RT (2006) Thermodynamics in materials science, 2nd edn. CRC, Boca Raton
Gaskell DR (2008) Introduction to the thermodynamics of materials, 5th edn. Taylor and Francis, New York
Hummel FA (1984) Phase equilibria in ceramic systems. Marcel Dekker, New York
McHale AE (1997) Phase diagrams and ceramic processes. Chapman and Hall, New York
Muan A, Osborn EF (1965) Phase equilibria among oxides in steelmaking. Addison-Wesley, Reading, Reference for experimental determination of phase diagrams in ceramics. Inspirational with very helpful commentary; a 'must see' text
Phase diagrams for ceramists, Vols. I–VIII. The American Ceramic Society, Columbus:
I (1964) edited by E.M. Levin, C.R. Robbins, and H.F. McMurdie
II (1969) edited by E.M. Levin, C.R. Robbins, and H.F. McMurdie
III (1973) edited by E.M. Levin and H.F. McMurdie

IV (1981) edited by R.S. Roth, T. Negas, and L.P. Cook
V (1983) edited by R.S. Roth, T. Negas, and L.P. Cook
VI (1987) edited by R.S. Roth, J.R. Dennis, and H.F. McMurdie
(Vols I–VI include mostly oxide and metal + oxide systems)
VII (1989) edited by L.P. Cook and H.F. McMurdie (Halide systems, many calculated diagrams with methods discussed)
VIII (1990) edited by B.O. Mysen (Geological, high pressure, and hydrothermal systems)
Under a new series title, but continuous numbering, *Phase Equilibria Diagrams, Vols. IX–XII*:
IX (1992) "Semiconductors and Chalcogenides," edited by G.B. Stringfellow
X (1994) "Borides, Carbides, and Nitrides," edited by A.E. McHale
XI (1995) "Oxides," edited by R.S. Roth
XII (1996) "Oxides," edited by A.E. McHale and R.S. Roth
Also a part of this series; *Phase Equilibrium Diagrams, Annuals'91,'92, and'93*, edited by A.E. McHale (The annuals contain a number of complex oxide systems.) and *Phase Diagrams for High T_c Superconductors*, edited by J.D. Whitler and R.S. Roth, (1991)
The books are too costly for most individuals and are now only produced as CDs (~$3000). If you are a PC user, you can check out the NIST Standard Reference Database 31 at http://www.nist.gov/srd/nist31.cfm or at the ACerS site; if you're a Mac user, bad luck.
Ragone DV (1994) Thermodynamics of materials, vol I. Wiley, New York
Swalin RA (1972) Thermodynamics of solids, 2nd edn. Wiley, New York

SPECIFIC REFERENCES

Ellingham HJT (1944) Reducibility of oxides and sulfides in metallurgical processes. J Soc Chem Ind (London) 63:125–133
Hazen RM (1999) The diamond makers. Cambridge University Press, Cambridge, Attaining the high pressures
Richardson FD, Jeffes JHE (1948) The thermodynamics of substance of interest in iron and steel making from 0°C to 2400°C. J Iron Steel Inst (London) 160:261–270
Saunders N, Miodownik AP (1998) CALPHAD (calculation of phase diagrams): a comprehensive guide. Pergamon, Oxford
Torres FC, Alarcón J (2004) Mechanism of crystallization of pyroxene-based glass-ceramic glazes. J Non-Cryst Sol 347:45–51

WWW

CALPHAD for CALculation of PHAse Diagrams. www.calphad.org. Available in many university libraries on line.
http://thayer.dartmouth.edu/icelab The site of the ice lab at Dartmouth
www.nist.gov/mml/ceramicsNIST's ceramics